

# Half-metallic electronic feature and thermophysical properties of the $\text{Ba}_2\text{CoMoO}_6$ perovskite-like cobalt molybdate

## Naturaleza electrónica espín-metálica y propiedades termofísicas del molibdato de cobalto tipo perovskita $\text{Ba}_2\text{CoMoO}_6$

Críspulo E. Deluque-Toro<sup>1</sup>, Arles V. Gil-Rebaza<sup>2,3</sup>, Jorge I. Villa-Hernández<sup>4a</sup>, David A. Landínez-Téllez<sup>4b</sup>, Jairo Roa-Rojas<sup>4c</sup>

<sup>1</sup>Grupo de Nuevos Materiales, Facultad de Ingeniería, Universidad del Magdalena, Santa Marta, Colombia.  
Orcid: 0000-0001-7792-3506. Email: deluquetoro@gmail.com

<sup>2</sup>Departamento de Física, Facultad de Ciencias Exactas (UNLP), Instituto de Física La Plata – IFLP, CONICET-CCT La Plata, La Plata, Argentina. Orcid: 0000-0001-8082-4576. Email: arvifis@gmail.com

<sup>3</sup>Grupo de Estudio de Materiales y Dispositivos Electrónicos (GEMyDE), Universidad Nacional de La Plata, Argentina.


<sup>4</sup>Grupo de Física de Nuevos Materiales, Departamento de Física, Universidad Nacional de Colombia, Colombia.  
Orcid: <sup>a</sup> 0000-0003-2713-0246, <sup>b</sup> 0000-0001-7108-617X, <sup>c</sup> 0000-0002-5080-8492.  
Emails: <sup>a</sup> jvillah@unal.edu.co, <sup>b</sup> dalandinezt@unal.edu.co, <sup>c</sup> jroar@unal.edu.co

Received: 10 April 2019. Accepted: 22 October 2019. Final version: 31 December 2019.

### Abstract

Perovskite-like materials which include magnetic elements have relevance due to the technological perspectives in the spintronics industry. In this work, the magnetic, structural and electronic properties of the  $\text{Ba}_2\text{CoMoO}_6$  double perovskite are investigated. Calculations are carried out through the Full-Potential Linear Augmented Plane Wave method within the framework of the Density Functional Theory with exchange and correlation effects in the Generalized Gradient and Local Density approximations, including spin polarization. From the minimization of energy as a function of volume using Murnaghan's state equation the equilibrium lattice parameter and cohesive properties of this compound were obtained. The study of the electronic structure was based in the analysis of the electronic density of states, and the band structure, showing that this compound evidences a conductive character for a spin channel and insulation for the other, and presents an integer value for the effective magnetic moment ( $3.0 \mu_B$ ), which allows it to be classified as a half-metallic material. The effects of pressure and temperature on thermophysical properties such as specific heat, Debye temperature, coefficient of thermal expansion and the Grüneisen parameter were calculated and analyzed from the state equation of the system. Obtained results reveal that, in the low-temperature regime, the specific heat at constant volume and pressure presents an analogous behavior to each other, with a tendency to the limit of Dulong-Petit typical of the structures of cubic perovskite-type, showing a value of  $246.3 \text{ J/mol.K}$  at constant volume and slightly higher values at constant pressure. The dependence of the thermal expansion coefficient, the temperature of Debye and the Grüneisen parameter with the increase in temperature are discussed in relation to other perovskite-like materials.

**Keywords:** complex perovskite; half-metallicity; electronic structure; equilibrium properties.

ISSN Printed: 1657 - 4583, ISSN Online: 2145 - 8456, CC BY-ND 4.0 

How to cite: C.E. Deluque Toro, A.V. Gil Rebaza, J.I. Villa Hernández, D.A. Landínez Téllez, J. Roa-Rojas, "Half-metallic electronic feature and thermophysical properties of the  $\text{Ba}_2\text{CoMoO}_6$  perovskite-like cobalt molybdate," *Rev. UIS Ing.*, vol. 19, no. 1, pp. 213-224, 2020. doi: 10.18273/revuin.v19n1-2020020

## Resumen

Los materiales de tipo perovskita que incluyen elementos magnéticos tienen relevancia debido a las perspectivas tecnológicas en la industria de la espintrónica. En este trabajo se efectúa un estudio exhaustivo de las propiedades magnéticas, estructurales y electrónicas de la perovskita doble  $\text{Ba}_2\text{CoMoO}_6$ . Los cálculos se realizan a través del método de ondas planas aumentadas y linealizadas dentro del marco de la teoría del funcional de la densidad con efectos de intercambio y correlación en las aproximaciones del gradiente generalizado y de densidad local, incluyendo polarización de espín. A partir de la minimización de la energía en función del volumen, utilizando la ecuación de estado de Murnaghan, se obtuvieron el parámetro de red de equilibrio y las propiedades cohesivas de este compuesto. El estudio de la estructura electrónica se basó en el análisis de la densidad electrónica de estados y la estructura de bandas, mostrando que este compuesto evidencia un carácter conductor para un canal de espín y aislante para el otro, presentando un valor entero para el momento magnético efectivo ( $3.0 \mu_B$ ), que permite clasificarlo como un material espín-metálico. Los efectos de la presión y la temperatura sobre las propiedades termofísicas, como el calor específico, la temperatura de Debye, el coeficiente de expansión térmica y el parámetro Grüneisen, se calcularon y analizaron a partir de la ecuación de estado del sistema. Los resultados obtenidos revelan que, en el régimen de baja temperatura, el calor específico a volumen y presión constantes presenta un comportamiento análogo entre sí, con una tendencia al límite de Dulong-Petit típico de las estructuras de tipo perovskita cúbica, mostrando un valor de  $246.3 \text{ J/mol.K}$  a volumen constante y valores ligeramente más altos a presión constante. La dependencia del coeficiente de expansión térmica, la temperatura de Debye y el parámetro Grüneisen con el aumento de temperatura se discute en relación con otros materiales de tipo perovskita.

**Palabras clave:** perovskita compleja; espín-metalicidad; estructura electrónica; propiedades de equilibrio.

## 1. Introduction

Perovskite-like ceramics with ideal formula  $\text{ABX}_3$ , wherein A represents alkaline earth and rare earth elements, B is a transition element cation and X is an anion, usually oxygen, evidence numerous physical properties which are particularly sensitive to inhomogeneities like distortions from their ideal cubic structure, vacancies and chemical substitutions [1]. One of these anomalies, which raises the complex perovskite with  $\text{A}_2\text{BB}'\text{O}_6$  formula, results from the ordering of B and B' cations on the octahedral site of the primitive perovskite unit cell.

The importance of complex perovskites is in the possibility of creating new magnetic materials  $\text{A}_2\text{BB}'\text{O}_6$ , with B and B' constituted by magnetic  $3d$  cations. Recently, the study of these materials has increased due to the possibility of applying them in the design and technology of magnetic devices for applications in high capacity magnetic information storage devices and RAM memories [2-3], prototypes for the transport of polarized currents [4], hard magnets [5], magnetic sensors [6], systems based on magnetic nanoparticles [7], among others. Likewise, during the last years, the calculations of first principles based on the Functional Theory of Density (DFT) have become a usual and very precise method for the theoretical prediction of diverse properties of perovskite-type materials, such as the crystallographic structure, electric transport mechanisms (considering the polarization of spin) and the distribution of valence electrons around

the Fermi level that allow characterizing the material as an insulator, semiconductor, conductor or half-metallic.

In addition, this type of calculation allows establishing the contribution of the different electronic orbitals to the magnetic and electrical properties, as well as the eventual ferroelectric response of the materials [8]. On the other hand, theoretical simulations have proved to be a very interesting method for the prediction of thermodynamic properties at high pressure, as a function of temperature, for perovskite-like materials [9]. This is possible because the macroscopic thermodynamic properties are strongly correlated with the microscopic dynamics of the atoms of the material. Thus, the collective vibrations of crystalline networks in solids take place in discrete packets of energy, or energy quanta, known as phonons.

This kind of fundamental excitations in solids, as well as the electrons, is responsible for the thermodynamic properties of materials. The most relevant role of phonons occurs for insulators and semiconductors, where they contribute directly to properties such as specific heat and thermal expansion, as well as their dependence on temperature. When speaking of phonons, it is assumed that the crystal vibrations are of harmonic character, which can be considered valid at low temperatures, more specifically below the Debye temperature of the solid. For this reason, theoretical methods are used as a complementary tool that allows the study of atomic dynamics at high temperatures, facilitating the calculation of the thermodynamic

properties of materials, through approximations such as the quasi-harmonic Debye model [10].

The results obtained through this method have been surprisingly close to the experimental values reported for some specific materials [11]. The growing interest for the double perovskite materials based on Co and Mo has to do with the tuning of the physical characteristics from its composition and the type of hybridizations of the electronic orbitals 3d and 4d, from which they can be generated properties that suggest its applicability in spintronics [12] and solid oxide fuel cells [13], among other modern technology devices.

From experimental results of the structural, electrical and magnetic behavior of the Ba<sub>2</sub>CoMoO<sub>6</sub> double perovskite were reported [14] and the authors claim that this material crystallizes in a cubic structure, belonging to the *Fm* $\bar{3}$ *m* (#125) space group. DFT calculations in this material with spin polarization revealed a conductor behavior for both up and down spin orientations when calculated by considering exchange and correlation potentials within the GGA and LSDA approximations [15].

In this work theoretical results of the structural and electronic characteristics of the double perovskite Ba<sub>2</sub>CoMoO<sub>6</sub> are reported, which have been made in the search of information that allows to infer the mechanisms responsible for the magnetic and transport properties of this material, through the analysis of the crystallographic parameters, the band structure, the density of electronic states, and the behavior of the specific heat, the thermal expansion, the Debye temperature and the Grüneisen parameter as functions of temperature and pressure.

## 2. Calculation method

It was used the Wien2k [16] within the framework of the Kohn-Sham Density Functional Theory (DFT) [17], applying the Full-Potential Linear Augmented Plane Wave method (FP-LAPW) and adopting the Generalized Gradient Approximation (GGA) for the exchange-correlation energy due to Perdew, Burke y Ernzerhof and also the Local Density Approximation (LDA) [18].

The self-consistent process in the numeric package Wien2k allows the total energy calculation for constituent elements and alloys.

Taking the experimental unit cell data as input, all the structures studied in this work were fully relaxed with respect to their lattice parameters and the internal

degrees of freedom compatible with the space group symmetry of the crystal structure. The resulting energies versus volume functions have been fitted to the equation of state due to Murnaghan [19] in order to obtain de minimum energy value, the bulk modulus, its pressure derivative and the equilibrium lattice parameters and associated volume.

The muffin-tin radius of the elements was 2.4, 1.8, 1.8 and 1.8 (in au) Ba, Co, Mo and O respectfully, angular momentum up to  $l = 10$  inside the muffin-tin sphere, a maximum vector in the reciprocal space of  $G_{MAX} = 12.0$ ,  $R_{MAX} = 7$ , and a mesh of 1500 points in the first Brillouin zone (equivalent to a maximum of 56 k points in the irreducible Brillouin zone). Finally, the convergence criteria for the self-consistent calculation were  $0.0001$  Ry for the total energies,  $0.0005$  u.a in the charge and  $1.0$  mRy/u.a. in the internal forces. Spin polarization was included in the calculations. The quasi-harmonic Debye model is applied in order to calculate the thermophysical properties of the material as a function of temperature, such as the specific heat at constant volume and pressure, the thermal expansion of the crystal, the Debye temperature and the Grüneisen parameter [20].

## 3. Results and discussion

A preliminary approach to the structure of a perovskite-type material can be made from the *SPuDS* structure prediction diagnostic software [21], which has been designed for this family of materials. Using this tool, it is possible to establish an approximate value of the network parameters of the crystal, which for this case was carried out considering the *Fm* $\bar{3}$ *m* (#225) space group. Then, using the code PowderCell (PCW) [22], the respective diffraction pattern was theoretically generated. The obtained picture, which is presented in figure 1, shows the characteristics of a perfect complex cubic structure.

The ideal double cubic perovskite A<sub>2</sub>BB'O<sub>6</sub> is characterized by the formation of a superstructure in which the cations B and B' are organized alternately along the crystallographic axes, coordinated with six oxygens that define the octahedral distribution of the structure. The presence of the superstructure can be determined by X-ray diffraction through the occurrence in the diffractogram of reflection peaks with indexes (311), (331), (511) and (531), which are observable in the theoretical diffraction pattern of figure 1.

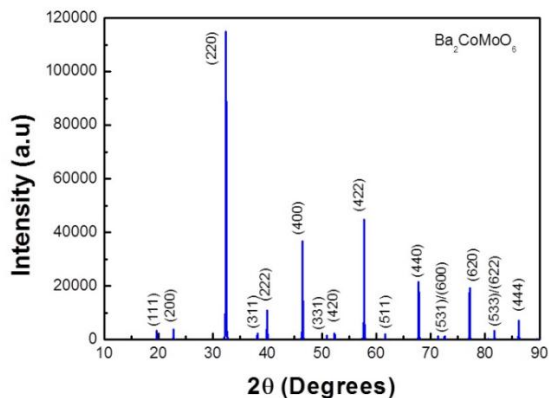


Figure 1. XRD simulated pattern for the  $\text{Ba}_2\text{CoMoO}_6$  complex perovskite obtained from the theoretical cell parameters. Source: Authors.

In the superstructure, the positions occupied by B and B' are not equivalent and for this reason the reflection lines mentioned above appear in the diffraction pattern [23]. In the case of the double cubic perovskite with formula  $\text{A}_2\text{BB}'\text{O}_6$ , when all the atoms are located in the ideal position, the intensity of the peaks, particularly of (111), is proportional to the difference in the scattering power of the atoms B and B' [24]. If the cations B and B' were located randomly in the structure, the peaks (111), (311), (331), (511) and (531) would have zero intensity, that is, they would not appear in the diffractogram. In that  $\text{Ba}_2\text{CoMoO}_6$  material, the order of the  $\text{Co}^{2+}$  and  $\text{Mo}^{6+}$  cations in positions B and B' can be clearly distinguished through the occurrence of the peaks mentioned above, whose intensities are significant.

The cell constant of  $\text{Ba}_2\text{CoMoO}_6$ , calculated from the simulation is  $a=7.8121 \text{ \AA}$ , which corresponds to 96.6% of the experimentally reported [14]. Figure 2 shows the ideal structure expected for this material. In the picture it is observed the  $\text{Co}^{2+}$  and  $\text{Mo}^{6+}$  cations adopt octahedral correlations with its nearest neighbors, consisting of  $\text{O}^{2-}$  anions. It is observed in figure 2, that the octahedra with  $\text{Co}^{2+}$  and  $\text{Mo}^{6+}$  are perfectly interspersed throughout the crystallographic structure, generating a salt-rock superstructure, according to the Miller planes.

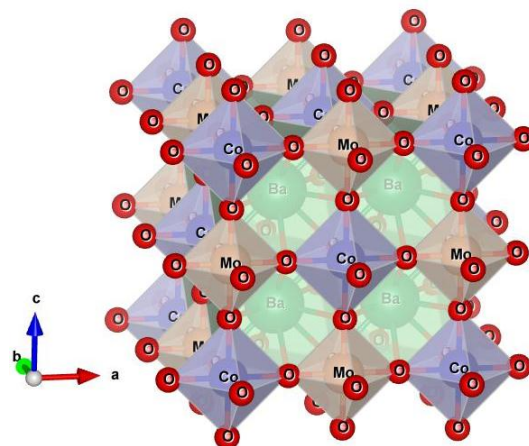


Figure 2. Crystalline structure of the  $\text{Ba}_2\text{CoMoO}_6$  complex perovskite for the  $Fm\bar{3}m$  (#225) space group. Source: Authors.

Figure 3 illustrates the energy as a function of volume. Each one of the squared points constitutes an individual calculation and the line corresponds to a fitting with the Murnaghan state equation, which was carried out by using the concept of the least-square fitting method [25]. The minimum of the energy is obtained for  $-44347.453444 \text{ Ry}$ , the volume modulus  $B_0 = 129.7 \text{ GPa}$ , and the equilibrium volume is  $485.358 \text{ \AA}^3$ . This value is close to that predicted from the *SPuDS*, which is  $476.764 \text{ \AA}^3$ . From the minimization of energy as a function of the volume of figure 3 within the GGA approximation it was calculated the lattice parameter  $a=7.8587 \text{ \AA}$ , which corresponds to 0.5% above the value predicted by the *SPuDS*. On the other hand, when the LDA approximation is used the equilibrium volume is  $387.8990 \text{ \AA}^3$ , which corresponds to a lattice parameter of  $a=7.293 \text{ \AA}$ , that turns out to be 7.0% different from the *SPuDS* prediction. This result is not uncommon considering that the application of LDA usually leads to an underestimation of the crystal lattice constants with respect to the GGA application, where the bulk lattice constants increase due to the presence of a more repulsive core-valence exchange [26]. In table 1 comparison between the atomic positions for the different theoretical procedures is showed.

Table 1.  $\text{Ba}_2\text{CoMoO}_6$  unit cell internal coordinates (Wyckoff positions) obtained from the *ab-initio* calculations using GGA and LDA exchange and correlation potentials. *SPuDS* data are included for comparison.

Atom	Wyckoff Site	GGA: (x,y,z)	LDA: (x,y,z)	SPuDS: (x,y,z)
$\text{Ba}^{2+}$	8c	0.2500, 0.2500, 0.2500	0.2500, 0.2500, 0.2500	0.2500, 0.2500, 0.2500
$\text{Co}^{2+}$	4a	0.0000, 0.0000, 0.0000	0.0000, 0.0000, 0.0000	0.0000, 0.0000, 0.0000
$\text{Mo}^{6+}$	4b	0.5000, 0.0000, 0.0000	0.5000, 0.0000, 0.0000	0.5000, 0.0000, 0.0000
$\text{O}^{2-}$	24e	0.2591, 0.0000, 0.0000	0.2589, 0.0000, 0.0000	0.2394, 0.0000, 0.0000

Source: Authors.

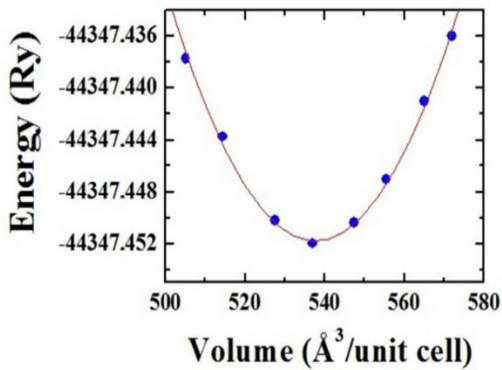


Figure 3. Minimization of the total energy as a function of volume for Ba<sub>2</sub>CoMoO<sub>6</sub> considering the *Fm* $\bar{3}m$  space group. Source: Authors.

Band structure calculations along high symmetry directions of the first Brillouin zone for the Ba<sub>2</sub>CoMoO<sub>6</sub> double perovskite are presented in figure 4 for the up and down spin configurations. In the picture, the energy of electrons as a function of wave vector *k*, along W-L- $\Lambda$ - $\Gamma$ - $\Delta$ -X-W directions is observed. From this figure, it is possible to infer that the Ba<sub>2</sub>CoMoO<sub>6</sub> material evidences a conductive character for a spin channel and an insulating nature for the other spin orientation, with a strong contribution of the 3*d* orbital of the Co cations in the valence band close to the Fermi level.

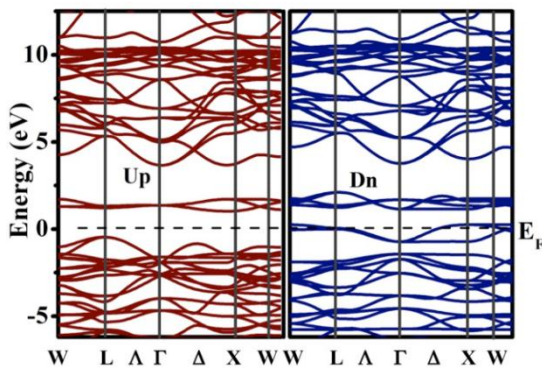


Figure 4. Band structure calculated for Ba<sub>2</sub>CoMoO<sub>6</sub> by considering both up and down spin polarizations. Source: Authors.

Partial DOS for Ba, Co, Mo and O atoms are presented in figure 5 for the up and down spin channels. It is observed in the pictures (figures 4 and 5) that the band structure is non-symmetrical around the Fermi level, which implies that there exists an effective magnetic moment. It was qualitatively determined orbitals Co-3*d* (*t*<sub>2*g*</sub>) are directly responsible for this response and the value of the effective magnetic moment was found to be 3.0  $\mu_B$ . The most relevant observation is relative to the

exotic property of half-metallicity, which is characterized by the differentiated conducting response of the spin up and spin down orientations, and an integer value of the effective magnetic moment. The density of states as a function of energy clearly evidences that the majority spin component shows an energy gap at the Fermi level, as the insulating materials, and the other spin orientation is continuous at the Fermi level, due to the strong hybridization of Co-3*d* (*t*<sub>2*g*</sub>) and O-2*p* states. On the other hand, it is observed that the crystalline field evidences a splitting between *t*<sub>2*g*</sub> and *e*<sub>g</sub> levels of Co-3*d*.

Exchange splitting between *t*<sub>2*g*</sub> up and *t*<sub>2*g*</sub> down, and between *e*<sub>g</sub> up and *e*<sub>g</sub> down are also observed. In general, the contribution of *t*<sub>2*g*</sub> states to DOS is significantly longer than *e*<sub>g</sub> states for both spin orientations. In figure 5, it was clearly observed the superposition of partial density of states for localized Mo *d-t*<sub>2*g*</sub> and delocalized Mo *d-e*<sub>g</sub> levels, which characterize the splitting of crystalline field between *t*<sub>2*g*</sub> and *e*<sub>g</sub> states, and exchange splitting between *t*<sub>2*g*</sub> up and *t*<sub>2*g*</sub> down levels, and between *e*<sub>g</sub> up and *e*<sub>g</sub> down states.

Figure 5 describes the exchange and crystalline field splitting behaviors of Co-3*d* and Mo-4*d* levels, respectively, for the Ba<sub>2</sub>CoMoO<sub>6</sub> compound. This result can be summarized by means of the qualitative scheme of figure 6, through the well-known Sarma model [27].

The left part of the figure describes the Co-3*d* states, where it is observed a strong exchange splitting between up and down spin configurations for both *e*<sub>g</sub> and *t*<sub>2*g*</sub> electronic states. Meanwhile, the splitting of the crystalline field is not as strong as the exchange splitting. On the other hand, Mo-4*d* levels are described on the right side of this diagram. It is interesting to note that states *e*<sub>g</sub> show energy values that are higher than those observed for the states of the Co. In addition, in the case of Mo, the exchange splitting cannot be observed because of the superposition between its *t*<sub>2*g*</sub> levels for the spin down configuration, while the crystalline field is significantly large. A clear scheme related to the hopping interactions, which are considered responsible for the hybridization of the Co-3*d* and Mo-4*d* states, can be consulted in C.M. Bonilla et al [28].

A fact of significant relevance is that the delocalized Co-*t*<sub>2*g*</sub> states for the spin-up orientations are located below the Fermi level, while the *t*<sub>2*g*</sub> states for the spin-down configuration are closer to the Fermi level. In this way, the shift of the spin-up and spin-down states induces a spin polarization of the mobile electrons due to the hopping interactions between the localized electrons and the conduction states. On the other hand,



for both spin up and spin-down orientations, the  $e_g$  states are strongly pulled down as a result of the hybridization, but these remain above the Fermi level.

In order to study the thermophysical properties of  $\text{Ba}_2\text{CoMoO}_6$ , this was considered that variations in pressure modify the thermodynamic response of materials. For this purpose, these properties were calculated as a function of temperature, under the application of several pressure values up to 35 GPa, using as a starting point the state equation, and following the quasi-harmonic approximation of the Debye model. [29]. In figure 7, the results of the specific heat at constant volume (figure 7(a)) and at constant pressure (figure 7(b)) as a function of the temperature up to  $T=1500$  K and under the application of pressures up to 35 GPa are exemplified. In these figures, it is possible to observe that the two curves show very similar behaviors in the low-temperature

regime (up to 400 K) for all the applied pressure values. It is clear from figure 7(a) that the specific heat at constant volume tends strongly to adopt a value independent of temperature (for very high-temperature values), in the regime known as the Dulong-Petit limit. This characteristic is observed for all applied pressure (up to 35 GPa) with a value for the Dulong-Petit limit of 246.3 J/mol.K. On the other hand, figure 7(b) reveals that this tendency is not universal for the case of specific heat at constant pressure. This occurs because at high temperatures it is expected that the quasi-harmonic model of Debye will fail, so that the divergences presented in figure 7(b) would not essentially constitute a response of the material [10]. Meanwhile, under the application of relatively low pressures (less than 20 GPa) a certain tendency towards a Dulong-Petit limit between 263.1 J/mol.K and 274.4 J/mol.K can be established.

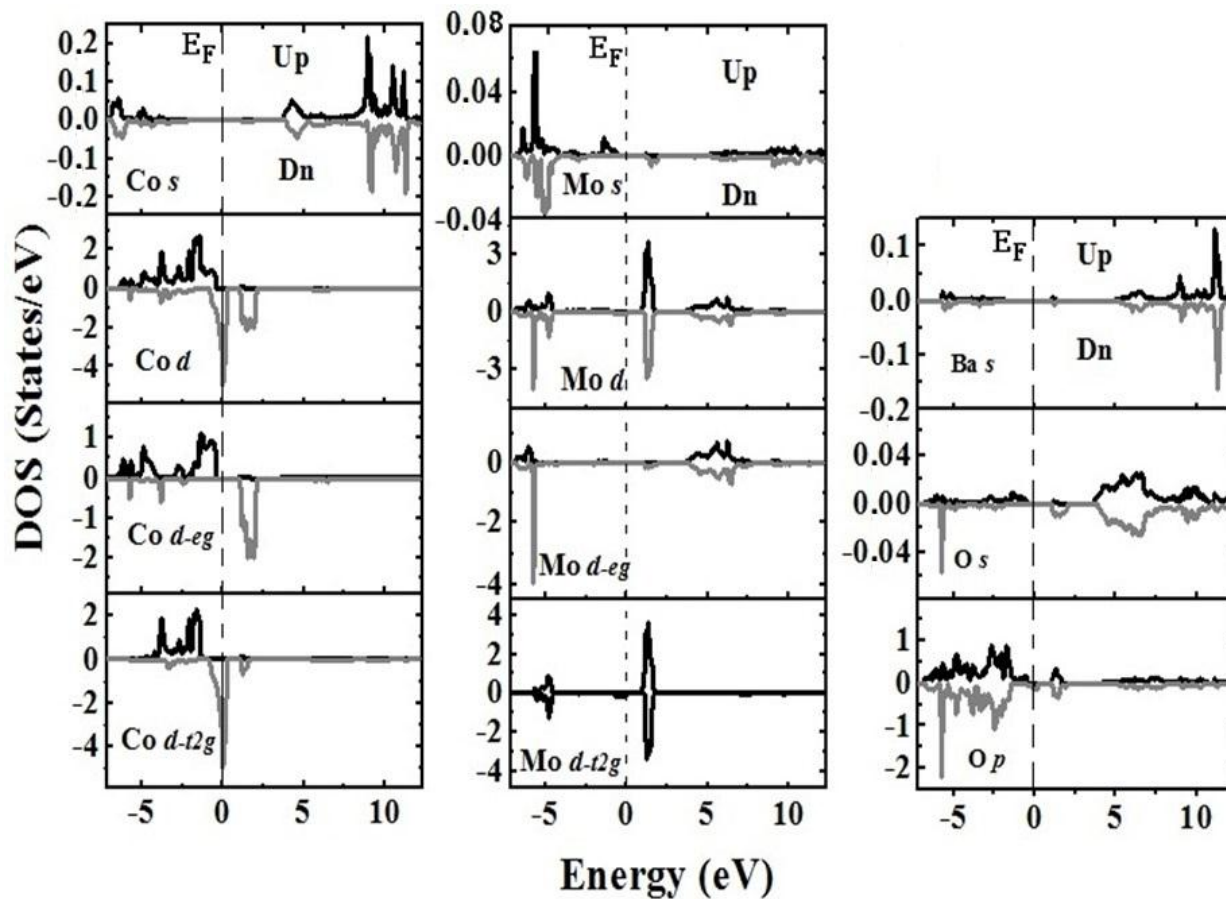


Figure 5. Partial DOS for Ba, Co, Mo and O atoms in the  $\text{Ba}_2\text{CoMoO}_6$  compound for both up and down spin orientations. Source: Authors.

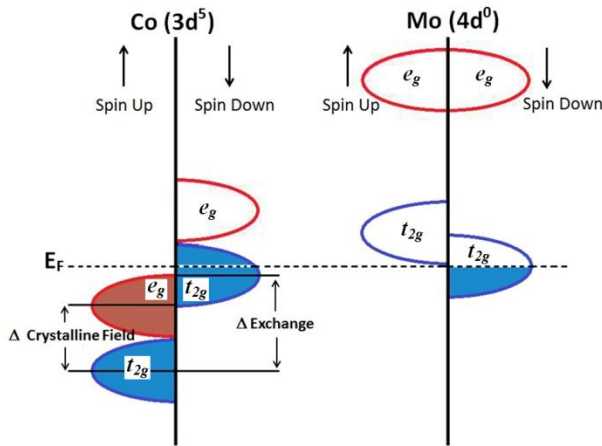


Figure 6. Spin distribution of the Co-d and Mo-d orbitals close to the Fermi level, which gives rise to half-metallic behavior. Source: Authors.

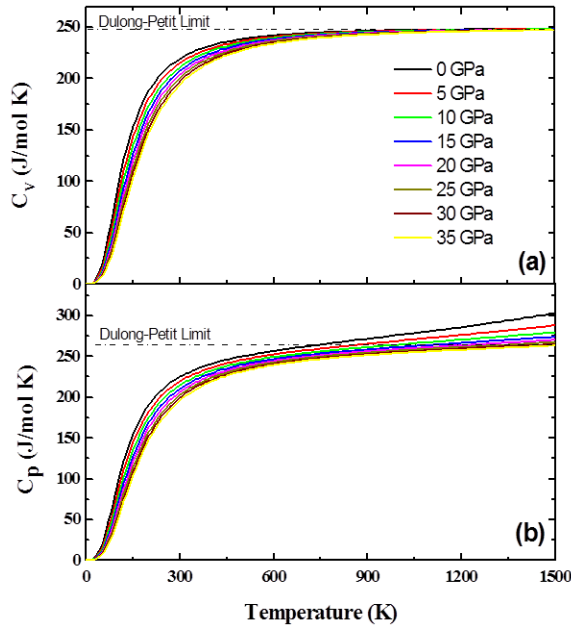


Figure 7. Specific heat  $C_V$  (a) and  $C_P$  (b) calculated through the Debye's quasi-harmonic model for the Ba<sub>2</sub>CoMoO<sub>6</sub> compound. Source: Authors.

These values agree with those reported for other double perovskites belonging to highly symmetric space groups [20]. Likewise, the predominance of a purely electronic response in specific heat is expected at low temperatures, while at high temperatures the phonics response should be predominant. The results of density of states and structure of bands presented in figures 4 and 5 reveal the majority presence of  $Co-3d-t_{2g}$  and minority orbitals  $4d-Mo-t_{2g}$  and  $2p-O$  in the vicinity of the Fermi level, which supplies the most relevant electronic contributions to the specific heat. On the

other hand, the contribution due to the  $6s-Ba$  orbitals is very incipient. In view of the foregoing, as the temperature of the material increases, the vibration of the cations and anions around their equilibrium positions, which results from the absorption of heat, makes an additional contribution to the total specific heat. In the case of the actual compound Ba<sub>2</sub>CoMoO<sub>6</sub>, some variations in the results may take place because of the polycrystalline character of this material, so that the specific heat must have dependencies of the porosity. This inference is made here because it is expected that the thermal energy needed to increase the temperature in denser materials is higher than in the more porous ones [30].

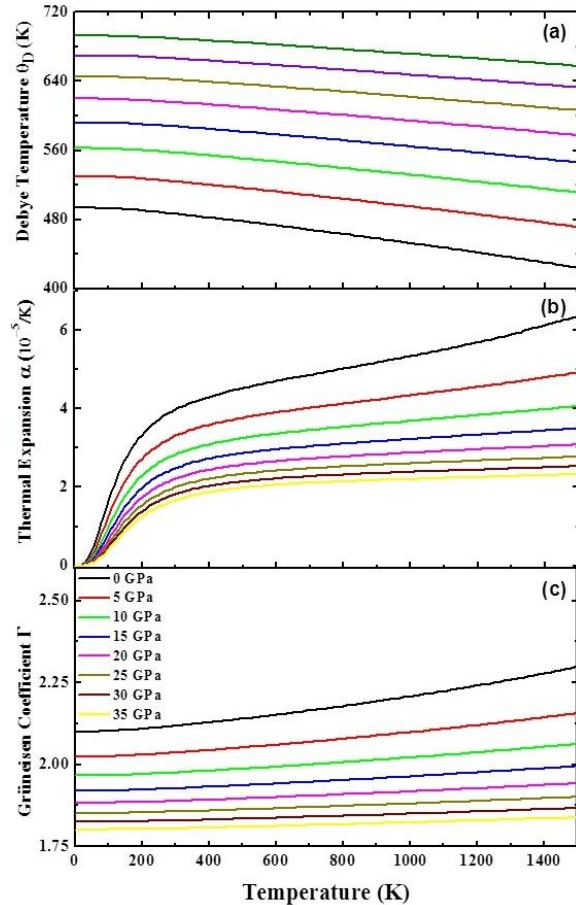


Figure 8. Debye temperature (a), thermal expansion coefficient (b) and Grüneisen parameter (c) calculated for the Ba<sub>2</sub>CoMoO<sub>6</sub> double perovskite. Source: Authors.

The Debye temperature as a function of temperature,  $\Theta_D(T)$ , was calculated for different pressure values (up to 35 GPa) as shown in figure 8(a). It is observed in the figure, that an increase in pressure produces a gradual increase in the elastic waves of the system, resulting in an increase in the temperature of Debye. The observed Debye temperature at  $T=0$  K is in the range between

494.4 K for  $P=0$  GPa and 693.3 K for  $P=35$  GPa. In the same way,  $\Theta_b(T)$  evidences a continuous non-linear decreasing behavior with the increase in temperature for all applied pressures, reaching values ranging from 424.8 K for  $P=0$  GPa to 660.5 K for  $P=35$  GPa (at  $T=1500$  K). A decrease of this type in  $\Theta_b(T)$  with the increase in temperature, accompanied by an increase with the growth of pressure has been reported for materials of double perovskite-type. [31].

The Debye temperature is understood as the highest value of temperature that can be obtained for a single normal vibration, for which it is possible to predict that the application of the pressure on  $\Theta_b(T)$  produces the effect of increasing the vibration frequencies of the bonds between the cations and the oxygen, i.e., octahedral bonds  $Co-O_6$  and  $Mo-O_6$ , and cuboctahedral  $Ba-O_{12}$  bonds. Therefore, the expansion of the structure due to the increase in temperature manifests itself as an increase in the wavelength of the vibrations, so that the frequency decreases, thus generating a decrease in the Debye temperature.

Figure 8(b) represents the dependence of the coefficient of thermal expansion,  $\alpha(T)$ , with the temperature under the application of different pressure values, up to 35 GPa. The picture shows a systematic decrease of  $\alpha(T)$  when the pressure is increased. This decrease is more pronounced at high temperatures, where a change can be perceived from  $6.4 \times 10^{-5} K^{-1}$  to  $2.3 \times 10^{-5} K^{-1}$  for a temperature of  $T=1500$  K. Likewise, it can be seen in the figure that at low temperatures, in the regime between 0 K and 200 K, the coefficient of thermal expansion increases abruptly when the temperature is increased. At  $T > 200$  K, this increase is smooth, reaching an approximately linear trend at very high temperatures. The  $Ba_2CoMoO_6$  material has a cubic structure, with its crystallographic parameters  $a=b=c$ , so that it has a perovskite-like nature corresponding to an isometric structure, so no large differences are expected in the values of thermal expansion as along the three crystallographic directions as would be expected for the case of more anisometric materials [32].

This behavior is correlated with the typical structural distortions of perovskite-type materials, where changes in temperature and pressure cause rotations and inclinations of the  $CoO_6$  and  $MoO_6$  octahedra, as well as elongations or compressions in certain directions of the crystallographic cell. Thus, the results obtained for  $\alpha(T)$  have to do with the types of distortion or structural transitions that are characteristic of the changes in temperature and pressure to which the material is subject. Therefore, it is expected that there will be possible differences between the theoretical results

presented in Figure 8b and the real experimental response that could be measured in the laboratory. The very low value of the coefficient of thermal expansion for this material suggests that it can be applied at low temperatures as material for fuel cell anodes [33].

The calculations carried out have not considered that the increase in temperature can give rise to structural phase transitions and that these transitions modify the response of the thermophysical properties under study. In figure 8(c) the Grüneisen parameter decreases gradually with the increase in applied pressure (from 2.10 for  $P=0$  GPa to 1.80 for  $P=35$  GPa, at  $T=0$  K). This behavior is observed for all temperatures that were considered in the calculations. In the meantime, it is also possible to see a continuous, smooth and non-linear growth of the Grüneisen parameter when the temperature is increased. At last, it can be stated that the behavior of the Grüneisen parameter as a function of temperature and pressure is a consequence of the variations produced in the vibration frequencies of the crystalline lattice, as previously discussed [34].

#### 4. Conclusions

It has performed several *ab initio* calculations over the  $Ba_2CoMoO_6$  double perovskite. Results show that it has an insulator behavior for the spin-up orientation and conductor for the spin-down configuration, as expected for half-metallic materials. Analysis of electronic structure for  $Ba_2CoMoO_6$  for both spin orientations permitted to infer that the  $t_{2g}$  spin-down states are responsible for the conductivity feature for both Co-3d and Mo-4d states. On the other hand, the insulating behavior of the spin-up configuration can be attributed to the  $e_g$  states. Additionally, it was correlated the results with the recent model propose to explain the conduction mechanism in this kind of compound by considering the Mechanism of Sarma for the magnetic interactions responsible for the magnetism on the  $Ba_2CoMoO_6$  double perovskites.

Another evidence of the half-metallicity is related to the integer value (in Bohr magneton) of the effective magnetic moment, which was determined to be  $3.0 \mu_B$ . It also has calculated the cell dimensions that minimize the total energy for each configuration using the Murnaghan equation state. The results of calculations of thermophysical properties through the application of the state equation, within the framework of the quasi-harmonic approximation of the Debye model, reveal that interatomic vibrations generate a small decrease in specific heat as a function of the applied pressure, with a tendency to the limit of Dulong-Petit, that presents values of the characteristic order of the highly



symmetric double perovskites. Additionally, it can be concluded that at temperatures lower than 400 K, the specific heats at constant volume and at constant pressure are very similar, which is justified by the low value of the coefficient of thermal expansion. On the other hand, the temperature of Debye increases with the increase in pressure and decreases with the increase in temperature. Conversely, both the coefficient of thermal expansion and the Grüneisen parameter decrease with pressure and increase slightly as a function of temperature.

In general, the behavior observed in thermodynamic properties is characteristic of double perovskite-type materials. It is important to note that the thermophysical properties depend strongly on the value of the Grüneisen parameter, since it is obtained from a third derivative of the state equation, which is why it is very sensitive to both the numerical errors in the derivation and the softness of the resulting curves. For this reason, the experimental measurement of these properties is very interesting to establish in a more objective way the microscopic mechanisms that originate them.

The scientific relevance of the current work, both in Colombia and in the world, takes place because the study of the electronic properties of this type of new materials allows to expand the general knowledge in science of new materials, suggesting the perspective of experimental investigations that contribute to the formation of highly qualified human resources that corroborates the theoretical predictions made here, also making possible the potential of their possible technological applications in spintronic devices.

### Acknowledgments

This work was partially financed by FONCIENCIAS, University of Magdalena and Departamento Administrativo de Ciencia y Tecnología Francisco José de Caldas – COLCIENCIAS, on the project FP80740-243-2019. One of us (J.I. Villa Hernández) received support by Departamento Administrativo de Ciencia y Tecnología “Francisco José de Caldas”, COLCIENCIAS, on the scholarship program for national doctorates.

### References

[1] C.J. Howard, B.J. Kennedy, P.M. Woodward, “Ordered double perovskites -- a group-theoretical analysis”, *Acta Cryst. B*, vol. 59, no. 4, pp. 463-471, 2003. doi: 10.1107/s0108768103010073

[2] L. Alff, in *Electron Correlation in New Materials and Nanosystems*, K. Scharnberg, S. Kruchinin (Eds.), *NATO Science Series II* 241, pp. 393-400, 2007.

[3] H. Sakakima, M. Satomi, E. Hirota, H. Adachi, “Spin-valves using perovskite antiferromagnets as the pinning layers”, *IEEE Transact. Magn.* vol. 35, no. 5, pp. 2958 – 29608, 1999. doi: 10.1109/20.801046

[4] T. Kimura, T. Goto, H. Shintani, K. Ishizaka, T. Arima, Y. Tokura, “Magnetic control of ferroelectric polarization”, *Nature*, vol 426, no. 6962 pp. 55-58, 2003. doi: 10.1038/nature02018

[5] J. M. De Teresa, J. M. Michalik, J. Blasco, P. A. Algarabel, M. R. Ibarra, C. Kapusta, U. Zeitler, “Magnetization of Re-based double perovskites: Noninteger saturation magnetization disclosed”, *Appl. Phys. Lett.* Vol. 90, 252514, 2007. doi: 10.1063/1.2751127

[6] L. Balcells, R. Enrich, A. Calleja, J. Sourcecuberta, X. Obradors, “Designing and testing of a sensor based on magneto resistive manganese perovskite thin film”, *J. Appl. Phys.* Vol. 80, no. 8, pp. 4298-4300, 1997. doi: 10.1063/1.364808

[7] Y. Mao, J. Parsons, J. S. McCloy, “Magnetic properties of double perovskite La<sub>2</sub>BmMnO<sub>6</sub> (B = Ni or Co) nanoparticles”, *Nanoscale*, vol. 5, no. 11, pp. 4720-4728, 2013. doi: 10.1039/c3nr00825h

[8] M. Bonilla, D.A. Landínez Téllez, J. Arbey Rodríguez, J. Albino Aguiar, J. Roa-Rojas, “Study of half-metallic behavior in Sr<sub>2</sub>CoWO<sub>6</sub> perovskite by ab initio DFT calculations”, *J. Magn. Magn. Mater.* Vol. 320, no. 14, pp. e397-e399, 2008. doi: 10.1016/j.jmmm.2008.02.179

[9] S.A. Dar, V. Srivastava, U.K. Sakalle, “Temperature and pressure dependent electronic, mechanical and thermal properties of f-electron based ferromagnetic barium neptunate”, *Chin. J. Phys.*, vol. 55, no. 5, pp. 1769-1779, 2017. doi: 10.1016/j.cjph.2017.08.002

[10] C.E. Deluque Toro, D.A. Landínez Téllez, J. Roa-Rojas, “Ab-initio analysis of magnetic, structural, electronic and thermodynamic properties of the Ba<sub>2</sub>TiMnO<sub>6</sub> manganite,” *Dyna* vol. 85, no. 205, pp. 27-36, 2018. doi: 10.15446/dyna.v85n205.68517

- [11] F. Guyot, Y. Wang, P. Gillet, Y. Ricard, "Quasi-harmonic computations of thermodynamic parameters of olivines at high-pressure and high-temperature. A comparison with experiment data", *Phys. Earth Planet. Int.* vol. 98, no. 1-2, pp. 17-29, 1996.
- [12] M. Bibes, A. Barthelemy, "Oxide spintronics", *IEEE Trans. Elec. Dev.* Vol. 54, no. 5, pp. 1003-1022, 2007.
- [13] Y-H. Huang, G. Liang, M. Croft, M. Lehtimäki, M. Karppinen, J.B. Goodenough, "Double-Perovskite Anode Materials  $\text{Sr}_2\text{MMoO}_6$  (M = Co, Ni) for Solid Oxide Fuel Cells," *Chem. Mater.*, vol. 21, no. 11, pp. 2319-2326, 2009. doi: 10.1021/cm8033643
- [14] M.J. Martinez-Lope, J.A. Alonso, M.T. Casais, M.T. Fernandez-Diaz, "Preparation, Crystal and Magnetic Structure of the Double Perovskites  $\text{Ba}_2\text{CoBO}_6$  (B = Mo, W)," *Eur. J. Inorg. Chem.*, vol. 2002, no. 20, pp. 2463-2469, 2002.
- [15] M. Musa Saad H.-E., M.A.K. Abdelhalim, A. El-Taher, "First-principles study of structural, electronic and magnetic properties of double perovskite oxides  $\text{Ba}_2\text{CoMO}_6$  (M=Mo and W)," *Mater. Sci. Semicond. Process.*, vol. 34, pp. 281-290, 2015. doi: 10.1016/j.mssp.2015.02.038
- [16] P. Blaha, K. Schwarz, G. K. H. Madsen, D. Kvasnicka, J. Luitz, WIEN2k, *An Aug-mented Plane Wave + Local Orbitals Program for Calculating Crystal Properties (Karlheinz Schwarz, Techn. Universität Wien, Austria, 2001)*, ISBN 3-9501031-1-2.
- [17] W. Khon, L. S. Sham, "Self-Consistent Equations Including Exchange and Correlation Effects," *Phys. Rev.*, vol. 140, pp. A1133-1138, 1965.
- [18] J.P. Perdew, K. Burke, M. Ernzerhof, "Generalized gradient approximation made simple," *Phys. Rev. Lett.*, vol. 77, no. 18, pp. 3865-3868, 1996.
- [19] F.D. Murnaghan, "The compressibility of media under extreme pressures," *Proc. Natl. Acad. Sci. USA*, vol. 30, no. 9, pp. 244-247, 1944.
- [20] C.E. Deluque Toro, A.S. Mosquera Polo, A.V. Gil Rebaza, D.A. Landínez Téllez, J. Roa-Rojas, "Ab Initio Study of the Electronic Structure, Elastic Properties, Magnetic Feature and Thermodynamic Properties of the  $\text{Ba}_2\text{NiMoO}_6$  Material," *J. Low. Temp. Phys.*, vol. 192, no. 5-6, pp. 265-285, 2018. doi: 10.1007/s10909-018-1937-9
- [21] M.W. Lufaso, P.M. Woodward, "Prediction of the crystal structures of perovskites using the software program SPuDS," *Acta Cryst. B*, vol. 57, no. 6, pp. 725-738, 2001.
- [22] W. Kraus, G. Nolze, POWDER CELL - a program for the representation and manipulation of crystal structures and calculation of the resulting X-ray powder patterns," *J. Appl. Crystallogr.*, vol. 29, no. 3, pp. 301-303, 1996.
- [23] Q. Madueño, D.A. Landínez Téllez, J. Roa-Rojas, "Production and characterization of  $\text{Ba}_2\text{NdSbO}_6$  complex perovskite as a substrate for  $\text{YBa}_2\text{Cu}_3\text{O}_{7-\delta}$  superconducting films," *Mod. Phys. Lett. B*, vol. 20, no. 8, pp. 427-437, 2006.
- [24] C.A. Triana, D.A. Landínez Téllez, J. Roa-Rojas, "General study on the crystal, electronic and band structures, the morphological characterization, and the magnetic properties of the  $\text{Sr}_2\text{DyRuO}_6$  complex perovskite," *Mater. Character.*, vol. 99, pp. 128-141, 2015.
- [25] R. Cardona, D.A. Landínez Téllez, J. Arbey Rodríguez M., F. Fajardo, J. Roa-Rojas, "Structural and magnetic properties of double-perovskite  $\text{Ba}_2\text{MnMoO}_6$  by density functional theory," *J. Magnet. Magnet. Mater.*, vol. 320, no. 14, e85-e87, 2008.
- [26] Y.M. Niquet, M. Fuchs, X. Gonze, "Exchange-correlation potentials in the adiabatic connection fluctuation-dissipation framework," *Phys. Rev. A*, vol. 68, pp. 032507, 2003.
- [27] D.D. Sarma, Sugata Ray, "Properties of a new magnetic material:  $\text{Sr}_2\text{FeMoO}_6$ ," *Chem. Sci.*, vol. 113, no. 5-6, pp. 515-525, 2001.
- [28] C.M. Bonilla, D.A. Landínez Téllez, J. Arbey Rodríguez, E. Vera López, J. Roa-Rojas, "Half-metallic behavior and electronic structure of  $\text{Sr}_2\text{CrMoO}_6$  magnetic system," *Phys. B*, vol. 398, no. 2, 208-211, 2007.
- [29] C.E. Alarcón Suesca, C.E. Deluque Toro, A.V. Gil Rebaza, D.A. Landínez Téllez, J. Roa-Rojas, "Ab-

initio studies of electronic, structural and thermophysical properties of the Sr<sub>2</sub>TiMoO<sub>6</sub> double perovskite,” *J. Alloys Compd.*, vol. 771, pp. 1080-1089, 2019. doi: 10.1016/j.jallcom.2018.08.314

[30] J. Kim, X. Chen, P-C. Shih, H. Yang, “Porous Perovskite-Type Lanthanum Cobaltite as Electrocatalysts toward Oxygen Evolution Reaction,” *Sustainable Chem. Eng.*, vol. 5, no. 11, pp. 10910-10917, 2017.

[31] O. Sahnoun, H. Bouhani-Benziane, M. Sahnoun, M. Driz, C. Daul, Comput., “Ab initio study of structural, electronic and thermodynamic properties of tungstate double perovskites Ba<sub>2</sub>MWO<sub>6</sub> (M= Mg, Ni, Zn),” *Mater. Sci.*, vol. 77, pp. 316-321, 2013. doi: 10.1016/j.commat.2013.04.053

[32] A. Fossdal, M. Menon, I. Wærnhus, K. Wiik, M-A. Einarsrud, “Crystal structure and thermal expansion of La<sub>1-x</sub>Sr<sub>x</sub>FeO<sub>3-δ</sub> materials,” *J. Amer. Ceram. Soc.*, vol. 87, pp. 1952-1958, 2004.

[33] Y. Markandeya, Y.S. Reddy, S. Bale, C.V. Reddy, Y. Bhikshamaiah, “Characterization and thermal expansion of Sr<sub>2</sub>Fe<sub>x</sub>Mo<sub>2-x</sub>O<sub>6</sub> double perovskites,” *Bull. Mater. Sci.*, vol. 38, no. 6, pp., 1603-1608, 2015.

[34] S.A. Dar, V. Srivastava, U.K. Sakalle, V. Parey, “Electronic structure, magnetic, mechanical and thermophysical behavior of double perovskite Ba<sub>2</sub>MgOsO<sub>6</sub>,” *Europ. Phys. J. Plus*, vol. 133, no. 64, 2018. doi: 10.1140/epjp/i2018-11889-y